Biochimica et Biophysica Acta 1828 (2013) 2099–2110

Contents lists available at SciVerse ScienceDirect

Biochimica et Biophysica Acta

journal homepage: www.elsevier.com/locate/bbamem

A combined fluorescence spectroscopy, confocal and 2-photon microscopy approach to re-evaluate the properties of sphingolipid domains

Sandra N. Pinto [a], Fábio Fernandes [a], Alexander Fedorov [a], Anthony H. Futerman [b], Liana C. Silva [c,*,1], Manuel Prieto [a,1]

[a] Centro de Química Física Molecular and Institute of Nanoscience and Nanotechnology, Instituto Superior Técnico, Universidade Técnica de Lisboa, Complexo I, Av. Rovisco Pais, 1049-001 Lisboa, Portugal
[b] Department of Biological Chemistry, Weizmann Institute of Sciences, Rehovot 76100, Israel
[c] iMed.UL, Research Institute for Medicines and Pharmaceutical Sciences, Faculdade de Farmácia, Universidade de Lisboa, Av. Prof. Gama Pinto, 1649-003 Lisboa, Portugal

ARTICLE INFO

Article history:
Received 21 March 2013
Received in revised form 10 May 2013
Accepted 13 May 2013
Available online 20 May 2013

Keywords:
Ceramide-platforms
Fluorescence spectroscopy and microscopy
Lipid rafts
Membrane lipid domains
Sphingolipids
2-photon microscopy

ABSTRACT

The aim of this study is to provide further insight about the interplay between important signaling lipids and to characterize the properties of the lipid domains formed by those lipids in membranes containing distinct composition. To this end, we have used a combination of fluorescence spectroscopy, confocal and two-photon microscopy and a stepwise approach to re-evaluate the biophysical properties of sphingolipid domains, particularly lipid rafts and ceramide (Cer)-platforms. By using this strategy we were able to show that, in binary mixtures, sphingolipids (Cer and sphingomyelin, SM) form more tightly packed gel domains than those formed by phospholipids with similar acyl chain length. In more complex lipid mixtures, the interaction between the different lipids is intricate and is strongly dictated by the Cer-to-Chol ratio. The results show that in quaternary phospholipid/SM/Chol/Cer mixtures, Cer forms gel domains that become less packed as Chol is increased. Moreover, the extent of gel phase formation is strongly reduced in these mixtures, even though Cer molar fraction is increased. These results suggest that in biological membranes, lipid domains such as rafts and ceramide platforms, might display distinctive biophysical properties depending on the local lipid composition at the site of the membrane where they are formed, further highlighting the potential role of membrane biophysical properties as an underlying mechanism for mediating specific biological processes.

1. Introduction

Over the past couple of decades, renewed attention has been given to membrane lipids. It is now widely recognized that lipids are more than mere structural components, participating actively in cellular processes as lipid second messengers [1,2], by interacting directly and specifically with certain proteins [3] and/or by providing specialized membrane regions (lipid domains) [4] that have the capacity to segregate or colocalize membrane proteins. The composition and physical properties of these membrane regions differ from the bulk membrane and are the key factor responsible for their specialized roles in biological processes, as in trafficking and signal transduction [5]. Several types of membrane domains have been identified including lipid rafts [6] and ceramide-platforms [7], which were shown to be important players in a number of cellular processes.

From a biophysical perspective, lipid rafts are characterized by their fluid ordered (liquid-ordered, l_o) nature [8] while Cer-platforms consist of more rigid domains with gel-like properties [9–12]. While there are some controversies regarding the existence of these domains in cellular membranes [13–15], it is nevertheless commonly accepted that regions with l_o-like properties might be present in biomembranes in a temporal- and spatial-dependent manner [16]. In contrast, the existence of gel domains under physiological conditions was a matter of dispute since their biophysical properties would limit diffusion of lipids and proteins in the biomembrane, which would compromise cell functioning [17]. However, it was recently shown that gel domains enriched in sphingolipids are present in the cellular membrane of yeast and that these might be involved in fundamental cell processes [18].

It has been hypothesized that alterations in membrane properties might be one of the trigger mechanisms for cellular responses and that minor changes in the properties of lipid domains might activate

Abbreviations: Cer, Ceramide; Chol, Cholesterol; DOPC, 1,2-dioleoyl-*sn*-glycero-3-phosphocholine; DPPC, 1,2-dipalmitoyl-*sn*-glycero-3-phosphocholine; DPH, 1,6-diphenyl-1,3,5-hexatriene; GUV, Giant unilamellar vesicles; Laurdan, 6-dodecanoyl-2-(dimethylamino)naphthalene; MLV, Multilamellar vesicles; l_d, Liquid disorder; l_o, Liquid ordered; NBD-DPPE, 1,2-dipalmitoyl-*sn*-glycero-3-phosphoethanolamine-*N*-(nitro-2-1,3-benzoxadiazol-4yl); POPC, 1-palmitoyl-2-oleoyl-*sn*-glycero-3-phosphocholine; PCer, N-palmitoyl-D-*erythro*-sphingosine; PSM, *N*-palmitoyl-*D*-erythro-sphingosylphosphorylcholine; Rho-DOPE, N-rhodamine-dipalmitoylphosphatidyl-ethanolamine; SLs, Sphingolipids; SM, Sphingomyelin; *t*-PnA, *trans*-parinaric acid

* Corresponding author. Tel.: +351 217 946 400x14204; fax: +351 217 937 703.
E-mail address: lianacsilva@ff.ul.pt (L.C. Silva).
[1] Co-senior authors.

0005-2736/$ – see front matter © 2013 Elsevier B.V. All rights reserved.
http://dx.doi.org/10.1016/j.bbamem.2013.05.011

specific cellular processes [19]. In this way, it is important to understand the physical properties underlying lipid domain formation and the characteristics of the phases that are formed. It is widely known that different lipids are able to form gel- and l_o-like phases. However, limited information is available regarding the differences in the properties of the lipid domains formed in membranes containing different lipid composition. In the present study, fluorescence spectroscopy, confocal and two-photon microscopy were used to further evaluate the characteristics of phases formed in different lipid mixtures that are known to present gel/fluid and/or l_o/l_d (liquid-disordered) phase separation. The use of model membranes that can be accurately manipulated, by changing the lipid components and their molar ratio, allowed the biophysical characterization of membranes composed of phospholipids, sphingolipids and/or cholesterol. Using a stepwise approach and a combination of fluorescent probes with different phase-related properties it was possible to identify i) the distinctive characteristics of the domains formed in those lipid mixtures and ii) the interplay between lipid rafts and Cer-platforms, giving further insights into the paradigm of Chol–Cer interactions.

2. Materials and methods

2.1. Materials

POPC (1-palmitoyl-2-oleoyl-*sn*-glycero-3-phosphocholine), DOPC (1,2-dioleoyl-*sn*-glycero-3-phosphocholine), DPPC (1,2-dipalmitoyl-*sn*-glycero-3-phosphocholine), PSM (*N*-palmitoyl-*D*-erythro-sphingosylphosphorylcholine), PCer (N-palmitoyl-D-*erythro*-sphingosine) and Rho-DOPE (N-rhodamine-dipalmitoyl-phosphatidylethanolamine) were from Avanti Polar Lipids (Alabaster, AL). Cholesterol (Chol) was from Sigma (Leiden, The Netherlands). DPH (1,6-diphenyl-1,3,5-hexatriene), *t*-PnA (*trans*-parinaric acid), Laurdan (6-dodecanoyl-2-dimethylaminonaphthalene) and NBD-DPPE (1,2-dipalmitoyl-*sn*-glycero-3-phosphoethanolamine-N-(7-nitro-2-1,3-benzoxa-diazol-4yl)) were from Molecular Probes (Leiden, The Netherlands). All organic solvents were UVASOL grade from Merck (Darmstadt, Germany). The concentration of the lipid and of the probes stock solutions was determined as described [20].

2.2. Fluorescence spectroscopy

Multilamellar vesicles (MLV) (total lipid concentration of 0.1 and 0.6 mM) were prepared as described [20]. The suspension medium was 10 mM sodium phosphate, 150 mM NaCl, and 0.1 mM EDTA (pH 7.4). Steady state fluorescence measurements of *t*-PnA, DPH and Laurdan (at a probe/lipid ratio of 1/500, 1/250 and 1/400, respectively) were performed in a SLM Aminco 8100 series 2 spectrofluorometer with double excitation and emission monochromators, MC400 (Rochester, NY). All measurements were performed in 0.5 cm × 0.5 cm quartz cuvettes. The excitation (λ_{exc})/emission (λ_{em}) wavelengths were 305/405 nm for *t*-PnA, 360/430 for DPH and 350/435 nm for Laurdan. A constant temperature was maintained using a Julabo F25 circulating water bath controlled with 0.1 °C precision directly inside the cuvette with a type-K thermocouple (Electrical Electronic Corp., Taipei, Taiwan). For measurements performed at different temperatures, the heating rate was always below 0.2 °C/min.

Laurdan GP (generalized polarization) was determined using [21]:

$$GP = \frac{I_{435} - I_{500}}{I_{435} + I_{500}} \quad (1)$$

where $I_{435\ and}\ I_{500}$ are the emission intensities at those wavelengths, corresponding to the maximum emission in the gel and in the liquid crystalline phase, respectively [21,22]. Theoretically this parameter varies from +1 to −1, however, experimentally it ranges from 0.7 to −0.3 both for pure lipids or mixtures e.g. [21–24].

Time-resolved fluorescence measurements with *t*-PnA were performed using $\lambda_{exc} = 305$ nm (using a secondary laser of Rhodamine 6G) and $\lambda_{em} = 405$ nm. The decays were analyzed using TRFA software (Scientific Software Technologies Center, Minsk, Belarus). The fluorescence decay is described by a sum of exponentials, where α_i is the normalized pre-exponential (or amplitude) and τ_i is the lifetime of the decay component *i*. The mean fluorescence lifetime is given by:

$$<\tau> = \sum_i \alpha_i \tau_i^2 / \sum_i \alpha_i \tau_i. \quad (2)$$

2.3. Determination of the partition coefficient of the probes between two phases

The partition coefficient of the probes (DPH, Laurdan, *t*-PnA) between gel and fluid ($K_p^{g/f}$) or liquid ordered and liquid disordered phases ($K_p^{lo/ld}$) in binary and ternary mixtures was determined from the variation of the photophysical parameters of these probes with the mole fraction of the fluid (f), X_f, the gel phase (g), X_g, the liquid disordered (l_d), Xl_d, and liquid ordered (l_o), Xl_o. The composition of the mixtures and the mole fraction of each phase (X_i) were taken from the tie-line at 23 °C of the respective phase diagram. The partition coefficient is an equilibrium constant that quantifies the partition of the probe between the two distinct phases present in these mixtures (f and g, l_o and l_d), and consequently is independent of the particular composition of the mixtures.

The partition coefficient was calculated according to the following expression [25]:

$$<r> = \frac{\varepsilon_g <r>_g K_p X_g + \varepsilon_f \overline{\tau}_f / \overline{\tau}_g <r>_f X_f}{\varepsilon_g K_p X_g + \varepsilon_f \overline{\tau}_f / \overline{\tau}_g X_f} \quad (3)$$

where X_i is the phase mole fraction, ε_i is the molar absorption coefficient, $\overline{\tau}_i$ and $<r>_i$ are the amplitude-weighted fluorescence lifetime and steady-state fluorescence anisotropy of the probe in phase *i*, respectively. K_p is obtained by fitting the equation to the data as a function of X_i.

2.4. Confocal fluorescence microscopy

Giant unilamellar vesicles (GUVs) containing the appropriate lipids and probes, were prepared by electroformation, as previously described [20]. A probe/lipid ratio of 1:500 for Rho-DOPE and 1:200 for NBD-DPPE and Laurdan was used. The GUVs were then transferred to 8 well Ibidi® μ-slides and confocal fluorescence microscopy was performed using a Leica TCS SP5 (Leica Microsystems CMS GmbH, Mannheim, Germany) inverted microscope (DMI6000) with a 63× water (1.2 numerical aperture) apochromatic objective. NBD-DPPE and Rho-DOPE excitation was performed using the 458 nm and 514 nm lines from an Ar^+ laser, respectively. The emission was collected at 480–530 nm and 530–650 nm, for NBD-DPPE and Rho-DOPE, respectively. Confocal sections of thickness <0.5 μm were obtained using a galvanometric motor stage. Two-dimensional (2D) projections were obtained using the Leica Application Suite-Advanced Fluorescence software.

Two photon excitation data were obtained by using the same Leica TCS SP5 inverted microscope but with a titanium-sapphire laser as the excitation light source. The excitation wavelength was set to 780 nm and the fluorescence emission was collected at 400–460 nm and 470–530 nm to calculate the GP images. Laurdan GP images were obtained through a homemade software based on a MATLAB environment. Briefly, both channel intensities are corrected for background intensities and Laurdan GP values are determined from:

$$GP = \frac{I_{400-460} - GI_{470-520}}{I_{400-460} + GI_{470-520}} \quad (4)$$

where $I_{400-460}$ and $I_{470-530}$ are the fluorescence intensities obtained at each acquisition channel and G is the calibration factor obtained from imaging Laurdan in ethanol using the same experimental conditions as those set for the lipid mixtures under study [26].

3. Results

3.1. Rationale for the selection of the probes and lipid mixtures

Several lipids have emerged as important signaling molecules involved in the regulation of cellular processes (e.g. [27]). Their mechanism of action might be related to the way they affect membrane biophysical properties [5]. In this study, we aim to characterize and compare the features of the domains formed by some of these lipids, particularly the sphingolipids SM and Cer, which are important players in the formation of rafts and Cer-platforms [28]. In addition, we aim to give further insight into the paradigm of Chol–Cer interactions and understand the interplay between lipid rafts and Cer-platforms. To this end, we have used a stepwise methodology starting from mixtures containing two (POPC/PSM and POPC/PCer), three (POPC/PSM/Chol) and up to four (POPC/PSM/Chol/PCer) lipid components with varying molar fractions. This stepwise strategy is fundamental to understand the phase behavior of the more complex mixtures and assign the type of phases formed, as previously shown by us [25,29]. We used a combined fluorescence spectroscopy, confocal and 2-photon microscopy multi-probe approach to evaluate the characteristics of the phases formed. As a comparative phospholipid model mixture we have used DOPC/DPPC, a binary mixture that displays gel/fluid phase separation and that was extensively characterized by other methods [22,30].

Concerning the fluorescent probes, we have identified in our previous studies a number of probes with particular phase preferences and photophysical behavior that together allow characterization of the different phases present in complex membranes: *t*-PnA is a suitable probe to evaluate the formation of gel phase [31]; NBD-DPPE has a higher preference for l_o domains and is mainly excluded from gel domains [32]; Rho-DOPE is only able to incorporate into a fluid (disordered) phase [32]; and DPH distributes equally between different phases, but is excluded from highly-ordered gel domains [11,20,33]. In addition, Laurdan was also used in this study to characterize the biophysical behavior of the mixtures. This probe has been shown to be highly sensitive to the physical state of the membranes (e.g. [21,23,34,35]). This sensitivity arises from dipolar relaxation processes that occur in the vicinity of the Laurdan molecule. In membranes, this phenomenon originates from the water molecules present in the bilayer in between the interface and the lipid chains [35]. In fluid membranes, the increased hydration together with the possibility of reorientation of the water molecules along the probe excited-state dipole leads to a decrease in the excited state energy and consequent red-shift of Laurdan emission maximum. On the contrary, in gel phase membranes the rate of relaxation is small and the hydration is low, resulting in a small emission spectral shift [35]. In addition, several reports suggest that Laurdan has an equal partition between gel, ordered and disordered phases [36], being an adequate probe to characterize the behavior of the different mixtures under study.

3.2. Biophysical characterization of phospholipid mixtures

The biophysical properties of DOPC/DPPC mixtures were revisited in the present study to: i) characterize the photophysical properties of the probes used and ii) use as a model phospholipid mixture to compare with our sphingolipid-containing lipid mixtures.

Thermotropic studies show that at low temperatures Laurdan GP is high indicating low water penetration and small dipolar relaxation, typical of membranes in the gel state. As the temperature is raised, GP values decrease due to increased membrane fluidity (Fig. 1A). This variation is more pronounced for mixtures containing higher DPPC content. This can be directly appreciated from the shift in the emission maximum of Laurdan emission spectra (Fig. S1), which indicates a change in the degree of hydration as temperature changes (Fig. S1A–S1E) and DPPC molar fraction is increased (Fig. S1F).

Measurements of Laurdan GP and fluorescence anisotropy provide complementary information regarding lipid packing (GP) and membrane fluidity (anisotropy) [22]. Laurdan GP (Fig. 1B) increases linearly with DPPC content, reflecting a progressive decrease in water penetration and increase in lipid packing. Laurdan anisotropy displays a tri-phasic behavior (Fig. 1C): i) below 30 mol% of DPPC the fluorescence anisotropy is typical of fluid phase and is insensitive to alterations promoted by increasing content of DPPC; ii) from 30-to-80 mol% of DPPC the fluorescence anisotropy increases linearly reflecting a decrease in membrane fluidity, which is due to the formation of a DPPC-enriched gel phase; iii) above 80 mol% of DPPC the membrane is already in a gel phase (e.g. [30]) and the fluorescence anisotropy of Laurdan is not further sensitive to an increase in lipid packing, in contrast to Laurdan GP which increases steadily as the membrane becomes enriched in DPPC.

DPH fluorescence anisotropy progressively increases with DPPC content in mixtures displaying gel-fluid phase coexistence (up to 75% DPPC [37]). Compared to Laurdan, DPH anisotropy variation is sharper and a plateau is attained for lower DPPC molar fractions. This is due to a higher preference of DPH for a DPPC gel phase, compared to Laurdan, as shown by its higher gel/fluid partition coefficient, $K_p^{g/f}$ (Table 1).

The properties of DOPC/DPPC mixtures were further studied by confocal and 2-photon fluorescence microscopy using 3 different probes (Figs. 2 and S2). Microscopy images of DOPC/DPPC GUVs labeled with NBD-DPPE/Rho-DOPE display gel/fluid phase separation (Fig. S2), in agreement with the reported phase behavior of these mixtures [30,38]. Gel domains are seen as dark regions due to the exclusion of both Rho-DOPE and NBD-DPPE. Analysis of Laurdan GP images in mixtures containing increasing content of DPPC (Fig. 2A–D) shows that both the fraction of ordered phase and the GP of the ordered regions increase with DPPC content. The comparison of GP values obtained in each mixture (Fig. 2E) shows that Laurdan GP in the fluid phase is low and mainly insensitive to the lipid composition. In contrast, GP in the gel phase is high and dependent on DPPC content, suggesting increased lipid packing in the gel phase. It is worth mentioning that the average GP values (determined over the whole vesicle for a population of GUVs) are comparable to those obtained by fluorescence spectroscopy (compare Figs. 1B and 2E). These values are an ensemble average of the GP values in the gel and in the fluid phase of all lipid vesicles and are therefore dependent on the fraction of each phase and on the partition of Laurdan into the different phases.

3.3. Biophysical properties of PSM-containing binary mixtures

For vesicles composed of PSM, both Laurdan GP and anisotropy efficiently report the gel-to-fluid transition of PSM (T_m ~ 40 °C) (Figs. 3A and S3), in agreement with the published value for this lipid [39]. In contrast, it was not possible to use these parameters to accurately determine the gel-to-fluid transition temperature of POPC/PSM mixtures containing up to 60 mol% of PSM because both Laurdan GP and anisotropy steadily decrease with temperature without a sharp variation that would correspond to the main transition temperature of these mixtures. Moreover, no significant changes in Laurdan anisotropy were observed in mixtures containing up to 60 mol% of PSM (Fig. 3B) and the values were significantly lower than those obtained in mixtures with phospholipids (Fig. 1C). On the other hand, re-plotting GP data as a function of PSM content (Fig. 3C) a progressive increase in GP is observed, reaching values typical of a gel phase in mixtures with higher PSM content. These results cannot be rationalized on the basis of the formation of a less ordered PSM enriched gel phase. In fact, the order of the PSM enriched gel phase is not expected to be smaller than the

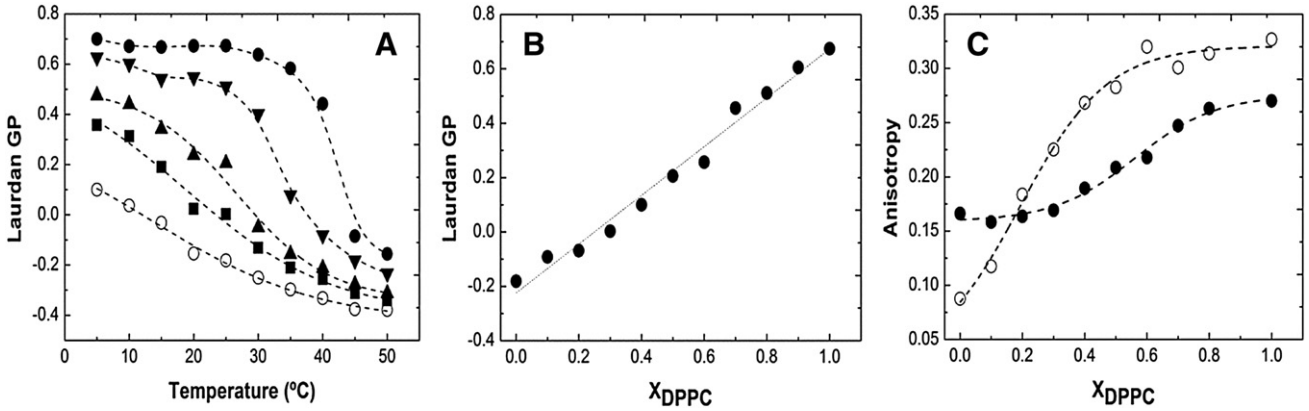

Fig. 1. Biophysical properties of DOPC/DPPC mixtures. In (A) the Laurdan GP was measured as a function of temperature in binary mixtures containing (○) 0, (■) 30, (▲) 50, (▼) 70 and (●) 100% of DPPC, respectively; and in (B) as function of DPPC molar fraction (solid circles). (C) Fluorescence anisotropy of Laurdan (closed circles) and DPH (open circles) as a function of DPPC molar fraction. The values are the means of independent experiments and standard deviation (SD) was always <1% (the error is within the size of the symbol).

order of DPPC gel phase, since analysis of Laurdan emission spectra shows a smaller red-shift in the emission maxima in PSM compared to DPPC (Fig. 3D), suggesting a smaller dipolar relaxation of the water molecules in PSM membranes. In this case, the absence of a sharp variation in the GP and fluorescence anisotropy values for Laurdan in the presence of gel/fluid phase coexistence is due to a lower partition coefficient of this probe (Table 1) into the PSM enriched gel phase. In this way, Laurdan becomes enriched in the fluid phase and is less sensitive to the formation of a PSM rich gel phase. This is further confirmed by two-photon microscopy where the increased packing of the PSM gel phase is shown by the higher GP in the gel phase (Figs. 2 and S3). The tight lipid packing might prevent the efficient partitioning of Laurdan into the PSM-gel phase resulting in a higher fraction of the probe reporting the properties of the fluid phase. Under these conditions the ensemble average GPs determined by fluorescence spectroscopy do not properly reflect the properties of the PSM gel phase because they are biased towards lower values (Table 1). Similar ensemble average GP values were obtained by microscopy (Fig. S3F) further supporting this hypothesis.

DPH and *t*-PnA were also used to characterize the properties of binary mixtures containing PSM (Fig. 3D). The fluorescence anisotropy of these probes increases with PSM content (Fig. 3D) showing that DPH and *t*-PnA are suitable probes to evaluate the properties of the PSM-enriched gel phase. The steeper increase in *t*-PnA anisotropy at lower PSM fractions is consistent with a higher partition of this probe into the gel phase (Table 1, [25]).

3.4. Biophysical properties of binary mixtures with PCer

We have previously shown that PCer forms highly-ordered gel domains that lead to the exclusion of probes that commonly partition into the gel phase, such as DPH (Table 1, [11]). Although extensive work was already carried out in these binary mixtures, their further characterization is justifiable due to the need of identifying the phase behavior of Laurdan in simpler mixtures before proceeding with the study of mixtures with more lipid components. Both Laurdan GP and anisotropy failed to report the gel-to-fluid transition of POPC/PCer mixtures (Fig. S4), probably due to a strong exclusion of the probe from the gel phase. This is further supported by the variation of GP (Fig. 4A) and anisotropy (Fig. 4B) as a function of PCer content. Increasing the PCer molar fraction led to a moderate increase in GP and anisotropy to values that are not typical of a gel phase [22,40] and which probably reflect a PCer-induced packing of the fluid phase [11] and/or a small incorporation of the probe in the gel phase. Further evidence for the exclusion of Laurdan from PCer-enriched gel domains arises from analysis of the Laurdan emission spectra (Fig. 4C). A progressive blue-shift in the emission maxima of Laurdan was observed for mixtures containing up to 30 mol% PCer, together with an increase in the intensity at 440 nm and a decrease in the fluorescence intensity of Laurdan at 480 nm. However, in mixtures containing higher PCer content, alterations in Laurdan emission spectra were accompanied by i) a decrease in the overall intensity of the probe, ii) a decrease in the fluorescence intensity at 440 nm and iii) a higher contribution of the intensity at 480 nm (Fig. 4C).

Two-photon microscopy experiments further confirmed the partial exclusion of Laurdan from PCer domains (Fig. 4D–E). The intensity of the probe in the gel phase is low, but the GP in the gel phase is relatively high, comparable to those obtained in POPC/PSM mixtures. This confirms the reduced water penetration in the membrane region where the probe is located due to its highly ordered nature.

3.5. Lipid rafts and ceramide domains

Five representative mixtures that display l_d-l_o phase coexistence were selected to study the properties of lipid raft-mimicking membranes. The

Table 1
Partition coefficients of the probes between l_o and l_d, $K_p^{lo/ld}$, and gel and fluid, $K_p^{g/f}$, phases.

Probe	$K_p^{lo/ld}$ in POPC/PSM/Chol[a]	$K_p^{g/f}$ in POPC/PSM[c]	$K_p^{g/f}$ in DOPC/DPPC	$K_p^{g/f}$ in POPC/PCer
t-PnA	0.82 ± 0.12	1.88 ± 0.14[d]	–	4.50 ± 0.60[f]
DPH	1.05 ± 0.08[b]	0.77 ± 0.08	1.83 ± 0.26[e]	~0[f]
Laurdan	0.62 ± 0.04	0.37 ± 0.11	0.79 ± 0.13[e]	~0[g]

The partition coefficients were determined from anisotropy variation (Eq. (3)).
[a] Determined using the diagram published in [48].
[b] Taken from [29].
[c] Determined using the diagram published in [48].
[d] Taken from [25].
[e] Determined using the phase diagram published in [37].
[f] Taken from [11].
[g] The photophysical parameters of Laurdan remain almost unchanged with PCer-gel fraction indicating that its partition into this phase is very low.

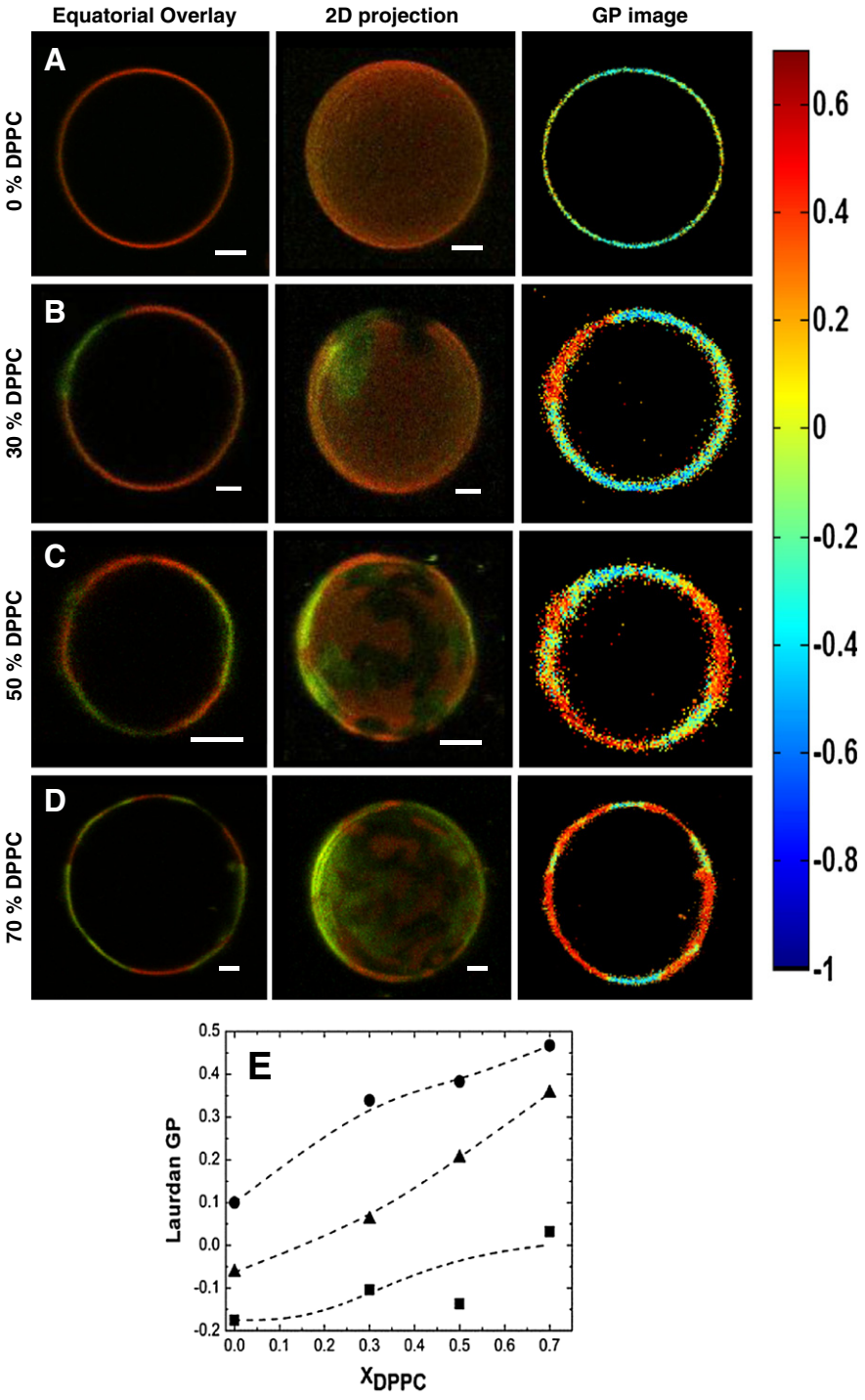

Fig. 2. Two-photon fluorescence microscopy of DOPC/DPPC mixtures. GUVs containing (A) DOPC and DOPC with (B) 30, (C) 50 and (D) 70 mol% of DPPC were labeled with Laurdan. Images from the left panel correspond to the overlay of equatorial *z*-section images taken with emission set at 400–460 nm (green channel) and 470–530 nm (red channel). Images from middle panel correspond to the overlay of 2D projection images taken with the same wavelengths described above. The GP images (right panel) were obtained by applying the GP function to the images from green and red channels pixel by pixel. The color scale is from −1 to 0.65. Scale bars correspond to 5 μm. (E) Variation of GP in the gel (circles), fluid (squares) and in the whole vesicle (triangles) as a function of DPPC content. At least 5 different GUVs were evaluated and GP values are the average of all GP images (equatorial *z*-sections) measured for each mixture. SD < 10%.

properties of these mixtures have been extensively characterized in our previous studies [29,33,41]. To evaluate PCer-induced changes in these membranes, PSM was partially replaced by PCer. The composition of the quaternary mixtures was selected taking into account our previous study, where PSM hydrolysis by sphingomyelinase was quantified over time [41]. In the present study the lipid composition used (Table 2) aims to mimic 30 min of PSM hydrolysis.

Analysis of the fluorescence anisotropy (Fig. S5A), mean fluorescence lifetime (Fig. 5A) and lifetime components (Figs. 5B and S5B–C) of the fluorescence intensity decay of *t*-PnA shows that replacement of PSM by PCer leads to an increase in *t*-PnA anisotropy and lifetime, consistent with the ability of PCer to form gel domains. These alterations are less pronounced in mixtures containing high Chol content due to solubilization of PCer in the Chol-enriched l_o phase [33,41]. It is

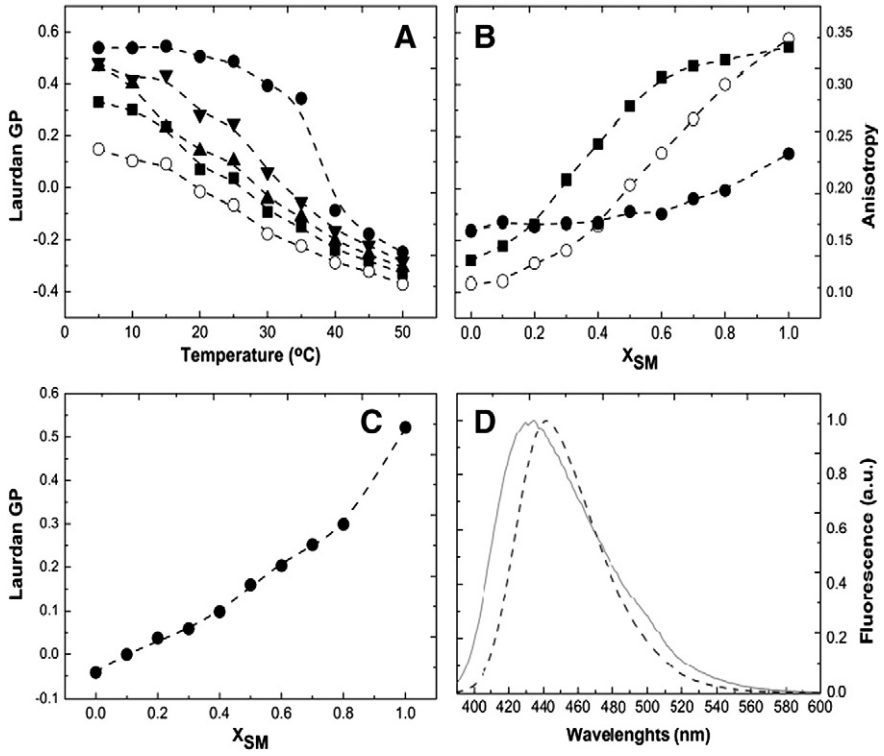

Fig. 3. Biophysical properties of POPC/PSM mixtures. In (A) the Laurdan GP was measured as a function of temperature in binary mixtures containing (○) 0, (■) 30, (▲) 50, (▼) 70 and (●) 100% of PSM, respectively. (B) Fluorescence anisotropy of (●) Laurdan, (○) DPH and (■) *t*-PnA as function of PSM molar fraction. The values are the average of at least three independent experiments and SD <0.01. (C) Laurdan GP variation as a function of PSM molar fraction. (D) Normalized fluorescence emission spectra of Laurdan in PSM (solid line) and DPPC (dashed line).

worth mentioning that in ternary mixtures, three exponentials describe the fluorescence intensity decay of *t*-PnA (Fig. S5B), in agreement with our previous report [29]. In the presence of PCer, i.e., quaternary mixtures, an additional lifetime component is required to describe the intensity decay of the probe (Fig. S5C). This new long lifetime component has been previously attributed to the formation of a PCer-enriched gel phase [29,41], suggesting that a gel phase coexists with other phase(s) in these quaternary mixtures. The longest lifetime component (τ_4) decreases as the content of Chol is increased in these mixtures (Figs. 5B and S5C), while the second longest (τ_3) increases, suggesting an interplay between the PCer-enriched gel phase and the Chol-enriched l_o phase. This interplay results both from changes in the packing of the phases, which are mainly reported by the lifetime components (τ_i) (Fig. 5B) and in the fraction of each of the phases, which can be qualitatively evaluated by the amplitude of the decay components (α_i) (Fig. 5C). As shown in Fig. 5B–C, the progressive decrease in the packing of the gel phase (τ_4) is accompanied by an increase both in the order (τ_3) and fraction (α_3) of the l_o phase. No significant variations were detected in the fraction of the gel phase (α_4). It should be noted that both the amplitude and lifetime components of the l_o phase of the quaternary mixtures follow a similar trend of variation as observed for the respective parameters in the ternary raft mixtures (Fig. 5B–C). The absolute values are however different, which might suggest differences in the packing of the l_o phase in ternary and quaternary mixtures.

The emission maximum of Laurdan shows a progressive blue shift with increasing Chol (and PSM) content of the ternary mixtures (Fig. 6A). This is consistent with a decrease in surface hydration as the l_o phase fraction is increased [29]. The values obtained in this study are in agreement with previous reports for similar lipid mixtures [42]. Replacement of PSM by PCer in the quaternary mixtures leads to an increase in Laurdan emission intensity at longer wavelengths (Figs. 6B and S6A) due to a partial exclusion of the probe from the PCer-gel phase, as described above. These spectral alterations are less pronounced in mixtures containing higher Chol content, further supporting the decreased ability of PCer to form tightly packed gel domains in membranes enriched in Chol [33,41]. Laurdan GP (Fig. 6C) and anisotropy (Fig. S6B) are always lower in quaternary mixtures compared to the ternary mixtures. The decrease in GP and anisotropy can be due to a partial exclusion of the probe from the PCer-enriched gel domains and/or to the decrease in the order of the lipid rafts due to PSM-depletion. To further elucidate this issue, confocal microscopy using NBD-DPPE/Rho-DOPE was performed (Fig. 7). NBD-DPPE displays a preferential partition into the l_o phase, while Rho-DOPE is excluded from this phase [33]. This is observed in the ternary mixtures, where the l_o phase fraction increases with Chol (Fig. 7A–D). The phase behavior of the quaternary mixtures is more complex and dependent on the composition of the mixtures. In mixtures containing lower Chol content, gel-fluid phase separation is observed (Fig. 7E–G), resulting in overlay images where gel domains (that exclude both probes) form dark areas in the bright (fluid) membrane. In quaternary mixtures containing higher Chol content (Fig. 7H), three phases are observed: i) gel domains, corresponding to the dark areas; ii) an l_o phase, that incorporates NBD-DPPE and iii) an l_d phase observed as red areas enriched in Rho-DOPE. Note that in mixtures with intermediate Chol content (Fig. 7G) some domains display a round-like shape from which narrow gel domains emanate. Domains displaying a round-like shape are typically formed upon l_o-l_d phase separation and are a result of low line tension [43]. In this particular case, the interface between the gel domains and the fluid phase seems to be stabilized by a thin layer of l_o phase that is observed as a faint green NBD-DPPE-enriched area surrounding these round-like domains. Interestingly, we have previously shown by fluorescence spectroscopy studies and FRET analysis that PCer forms gel domains that become surrounded by an l_o phase in raft-containing Cer mixtures [29]. This is now visually confirmed in the present study.

Analysis of Laurdan GP by two-photon microscopy (Fig. 8) further confirms the formation of a distinct phase in the quaternary mixtures. However, the results suggest that only two phases coexist in the

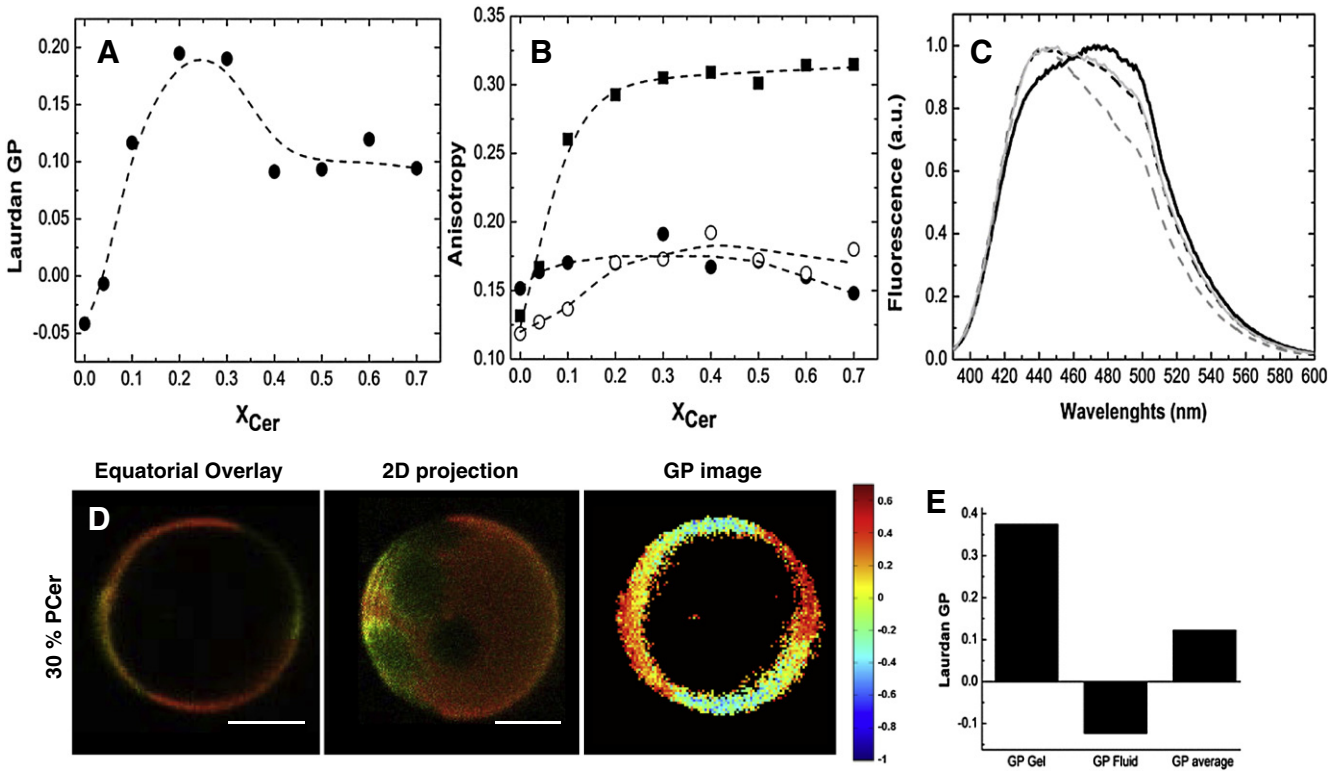

Fig. 4. Biophysical properties of POPC/PCer mixtures. (A) Laurdan GP as a function of PCer molar fraction. (B) Fluorescence anisotropy of (●) Laurdan, (○) DPH and (■) *t*-PnA as a function of PCer content. The values are the means of independent experiments and SD <0.01. (C) Laurdan emission spectrum in (solid black line) POPC and POPC-containing (grey dashed line) 30, (grey solid line) 50 and (black dotted line) 70 mol% of PCer. (D) Two-photon fluorescence microscopy images of POPC/PCer 70:30 GUVs labeled with Laurdan. Images from the left panel correspond to the overlay of equatorial *z*-section images taken with emission set at 400–460 nm (green channel) and 470–530 nm (red channel). Images from middle panel correspond to the overlay of 2D projection images taken with the same wavelengths described above. The GP images (right panel) were obtained by applying the GP function to the images from green and red channels pixel by pixel. The color scale is from −1 to 0.65. Scale bars correspond to 5 μm. (E) GP values in the gel, fluid and in the whole POPC/PCer 70:30 vesicle. At least 5 different GUVs were evaluated and GP values are the average of all GP images (equatorial *z*-sections). SD < 10%.

quaternary mixtures: gel/fluid for low to intermediate Chol content (Fig. 8E–G) and gel/l_o for high Chol content (Fig. 8H). These apparently contradictory results are probably a consequence of the strong photoselection of Laurdan molecules, particularly when located within the ordered phases (e.g. [40]). This might compromise the accurate detection of the 3 phase regions observed by the combination of the fluorophores NBD-DPPE/Rho-DOPE (Fig. 7). The existence of a gel-like phase in the quaternary mixtures is however clear, which is seen as darker narrow areas in the bright membranes. Even though a stronger photoselection effect is expected for gel domains located in the pole region of the vesicle, the extremely low intensity arising from these regions might further suggest the low incorporation of Laurdan into these gel domains. Determination of the GP values in the ordered regions of the membrane further supports this hypothesis because there are essentially no differences in the GP of the ordered regions from the ternary and quaternary mixtures (Fig. 8I). In addition, the fraction of gel domains present in the quaternary mixtures is small which precludes an accurate determination of the GP of the gel phase. Accordingly, the retrieved values reflect mainly the GP of l_o phase, suggesting that the l_o phase is similar in ternary and quaternary mixtures. However, differences in the properties of l_d phase are observed: the GP of the fluid phase is lower in quaternary mixtures containing higher Chol content (Fig. 8I). This is probably associated with the alteration in the composition of the phases, as discussed below.

Table 2
Lipid composition (X_{lipid}) of the ternary (POPC/PSM/Chol) and quaternary (POPC/PSM/Chol/PCer) mixtures used in the present study.

Ternary			Quaternary			
X_{POPC}	X_{PSM}	X_{Chol}	X_{POPC}	X_{PSM}	X_{Chol}	X_{PCer}
0.80	0.20	0.00	0.80	0.13	0.00	0.07
0.72	0.23	0.05	0.72	0.12	0.05	0.11
0.60	0.26	0.14	0.60	0.13	0.14	0.13
0.45	0.30	0.25	0.45	0.14	0.25	0.16
0.34	0.33	0.33	0.34	0.14	0.33	0.19
0.25	0.35	0.40	0.25	0.14	0.40	0.21

4. Discussion

4.1. Phase behavior of the probes

Our previous studies have already highlighted the importance of using a multiprobe approach to study membrane biophysical properties by fluorescence spectroscopy and microscopy. In the present study, additional evidence was obtained. We selected several different lipid mixtures that display distinct phase behavior and performed an extensive characterization using different fluorescent probes. Some of these probes, such as DPH and Laurdan, are commonly ascribed as good probes to report the biophysical properties of the membranes due to their ability to partition equally between different phases [30,44]. We have now demonstrated that their phase behavior depends on the type of phase and, in particular, on the lipid composition of the phase. Table 1 summarizes the partition behavior of the probes for the studied mixtures. We show that $K_p^{g/f}$ changes depending on the type of lipid that is involved in the formation of the gel phase. A $K_p^{g/f}$ above 1 denotes a preference towards the gel phase, while values below 1 show a preferential incorporation of the probe in the fluid phase. A higher partition of DPH and Laurdan into DPPC gel domains was observed compared to a PSM gel phase. Partitioning of these probes into PCer-gel domains was virtually

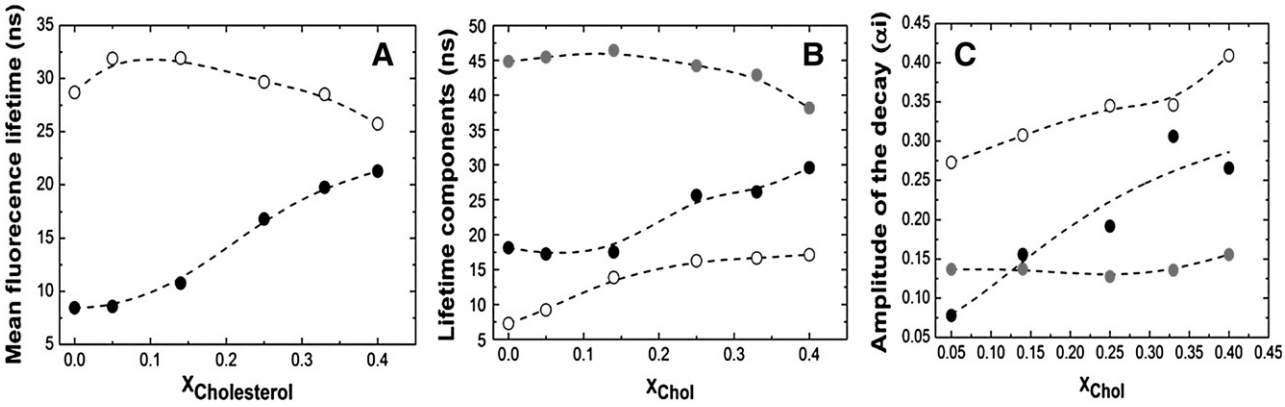

Fig. 5. Ceramide-induced biophysical changes in lipid raft mixtures. *t*-PnA fluorescence lifetime was measured in ternary POPC/PSM/Chol and quaternary POPC/PSM/Chol/PCer mixtures and the (A) mean fluorescence lifetime, (B) long lifetime components of *t*-PnA fluorescence intensity decay and (C) amplitude of the decay components were represented as a function of Chol molar fraction. In (A) the *solid symbols* correspond to ternary mixtures while *open symbols* to quaternary mixtures (see Table 2 for the composition of the mixtures). In (B,C) the longest lifetime component (τ_3) and its amplitude (α_3) of the ternary mixtures are shown in black. For the quaternary mixtures the two longest lifetime components and respective amplitudes are shown in white (τ_3, α_3) and light grey (τ_4, α_4). See text for further details. The values are the means of independent experiments and SD <2%.

non-existent. By comparing the different extent of incorporation of the probes into a gel phase formed by the different lipids, it is possible to infer their distinct packing properties. Partial exclusion of a probe from a gel phase suggests an increase in the packing of the lipids which is no longer suitable to accommodate a bulkier molecule.

It should also be noted that knowledge about the partition behavior of the probes is essential when evaluating parameters obtained by bulk methodologies, such as fluorescence spectroscopy. For instance, without knowing the $K_p^{g/f}$ of Laurdan in POPC/PSM mixtures, analysis of the data in Figs. 1 and 3 would suggest that PSM gel domains were less-ordered than those formed by DPPC. Analysis of fluorescence microscopy data is less critically dependent on the quantitative partitioning of the probes, since information can be retrieved directly from image analysis. Nevertheless, a lower partition will correspond to lower intensity of the probe in these membrane regions. This imposes difficulties when working with probes such as Laurdan, where GP values are recovered from the analysis of the intensities of images obtained in two different channels. Another disadvantage can be anticipated, which results from the utilization of these probes in complex cell membranes, where the lower incorporation of the probe into certain lipid phases might preclude their identification.

Performing studies with multiple probes displaying different phase behavior is therefore highly advantageous, particularly for characterizing systems presenting multiple phases and/or complex phase behavior. As shown in this study it was possible to identify differences in the characteristics of the phases simply by analyzing the photophysical parameters of the different probes. It should however be stressed that a combined fluorescence spectroscopy and microscopy approach provides deeper insight into the biophysical properties of the different lipid mixtures.

4.2. Sphingolipids form tightly-packed gel domains

The results obtained in the present study show that the packing of gel domains formed in binary mixtures increases in the order DPPC < PSM < PCer. Evidence for this was obtained by changes in the fluorescence anisotropy and lifetime of the different probes and in the microscopy data, particularly the GP of Laurdan in the gel phase. In addition, the difference in the partitioning of the probes into PSM and DPPC gel phases must be related to differences in the packing properties of the domains formed by these lipids [11]. Previous studies (e.g. [45]) have shown that Laurdan GP was lower in ganglioside gel phase micelles than in DPPC and, in addition, Laurdan emission spectrum displayed a red-shift. The authors suggested that the extent of water dipolar relaxation around the excited probe was dependent on the size of the polar headgroup, and that the larger the headgroup, the higher the dipolar relaxation due to increased water content at these interfaces. In our study, the ensemble average GP decreases in the order DPPC > PSM > PCer. DPPC and PSM display the same headgroup and PCer has a very small headgroup. Accordingly, our results are not

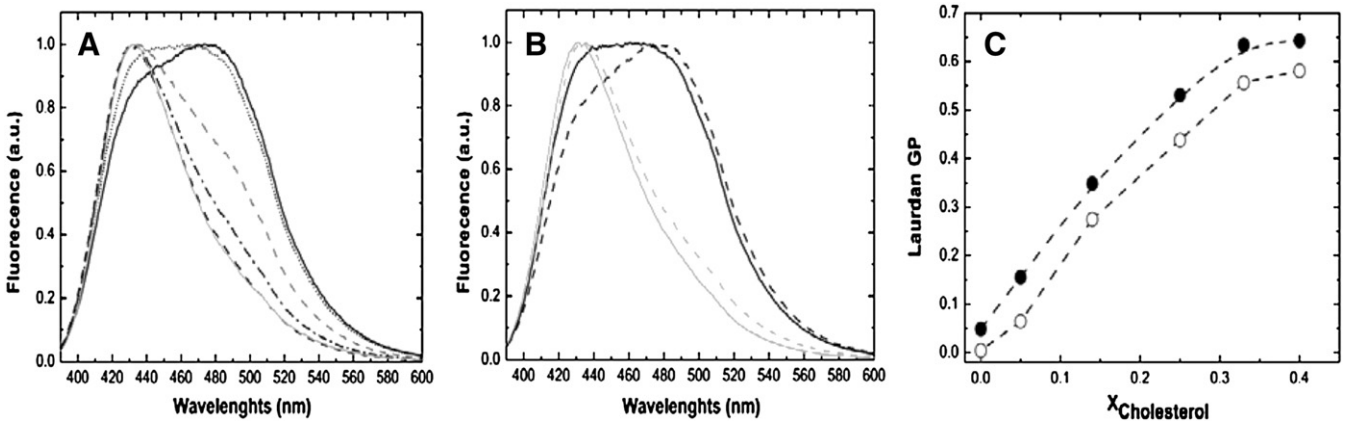

Fig. 6. Laurdan fluorescence spectroscopy as a tool to evaluate the interplay between ceramide and lipid rafts. (A) Normalized emission spectra in ternary mixtures containing (solid black line) 0, (dark grey solid line) 5, (dashed light grey line) 14 (dashed light grey line) 25, (dashed dot black line) 33 and (solid light grey) 40 mol% of Chol. (B) Normalized Laurdan emission spectra in (solid lines) ternary and (dashed lines) quaternary mixtures containing (black line) 5 or (light grey) 40 mol% of Chol. (C) Variation of Laurdan GP in (●) ternary and (○) quaternary mixtures as a function of Chol content. The values are the means of at least three independent experiments and SD <2%.

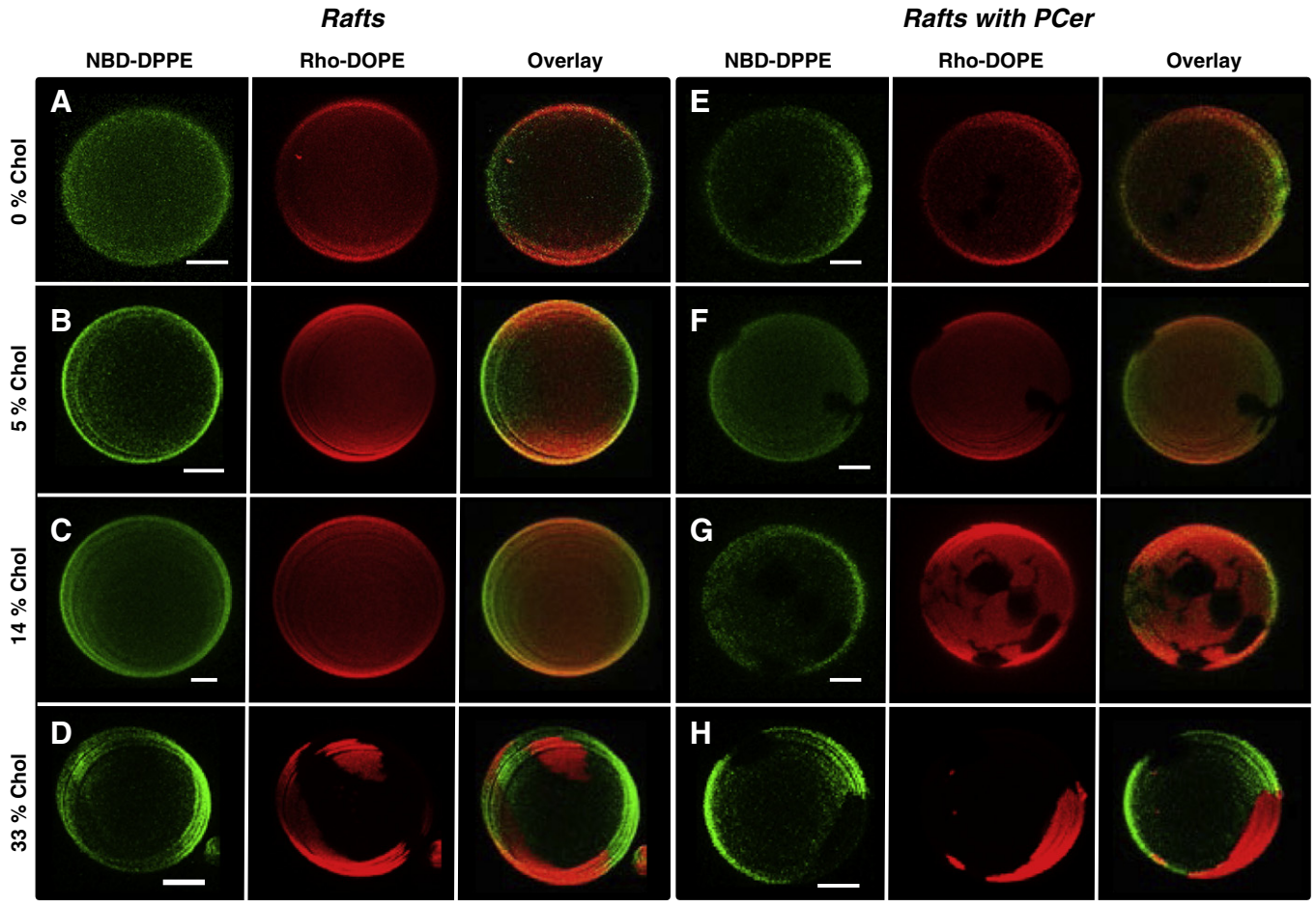

Fig. 7. Confocal fluorescence microscopy of ternary POPC/PSM/Chol and quaternary POPC/PSM/Chol/PCer mixtures. 2D projection images of (A–D) ternary and (E–H) quaternary mixtures were obtained from 0.4 μm confocal slices of GUVs labeled with NBD-DPPE (green channel) and Rho-DOPE (red channel). The GUVs were formed with (A,E) 0, (B,F) 5, (C,G) 14 and (D,H) 33 mol% of Chol. The overlay images are shown in yellow. Scale bars correspond to 5 μm.

explained by the hypothesis raised by the authors [45]. Moreover, the emission spectra of Laurdan in PSM and PCer do not display a red-shift, as observed for gangliosides [45]. In contrast, the emission maxima move towards lower wavelength (higher energy) in PSM membranes (Fig. 3C) suggesting decreased hydration and higher lipid packing despite the lower ensemble average GP values. In addition, the GP of the gel phase (as determined by two-photon microscopy) is always higher in PSM membranes independent of the fraction of the gel phase (Fig. 9A). In this way, in some cases Laurdan GP values offer incomplete information on the level of ordering in a membrane.

The increased packing of sphingolipid-containing mixtures is due to extensive H-bonding since these lipids can act both as donors and acceptors for H-bonding, in contrast to DPPC. A recent study using Di-4-ANEPPS, a probe that displays intermediate membrane depth, near the region of the carbonyl or amide group, revealed decreased hydration in PSM compared to DPPC [46]. The authors pointed out that the reduced hydration can be accompanied by a reorientation of the headgroup, particularly in the case of the gel phase. DPPC forms a more tilted gel phase than PSM [47] which can account for the different hydration. Compared to PCer, PSM has a bulkier polar headgroup which might prevent the closer packing of the lipid chains. A tighter packing of the PCer-gel can also be inferred by the longer lifetime component of *t*-PnA fluorescence intensity decay that increases up to ~50 ns with as little as 20 mol% of PCer, compared to PSM gel where long lifetime component (~40 ns) is obtained for PSM molar fractions close to 100% of gel phase [48] (Fig. 9B). These results are in agreement with recent conclusions taken from surface rheology studies performed on egg Cer monolayers [49,50]. In these studies it was shown that at surface pressures mimicking the biological membranes, Cer monolayers are very rigid solid assemblies, stiffer than other solid-like lipid systems.

4.3. Lipid rafts and ceramide-domains

Understanding the properties of lipid rafts and Cer-domains is one of the biophysical questions with the highest biological relevance. Moreover, understanding the interaction of Cer with lipid rafts is of utmost importance because it has been postulated that upon stress stimuli Cer is formed in the plasma membrane through hydrolysis of SM present in lipid rafts (e.g. [51]). Our results confirm the stronger effect that PCer has on the biophysical properties of lipid rafts containing lower Chol content. The fluorescence lifetime of *t*-PnA clearly shows that PCer forms gel-domains and their order decreases as Chol content is increased. This is shown by the decrease in the long lifetime component of *t*-PnA intensity decay in quaternary mixtures containing higher Chol content. Note that the *t*-PnA lifetime component is extremely long in all quaternary mixtures further supporting the highly-ordered nature of PCer-gel domains. The decrease in the packing is probably related with the composition of the gel phase that might have a substantially higher content of the remaining lipid components. This could only be assessed by a thorough characterization of the quaternary mixtures and respective phase diagram, which is out of the aim of this work. Nevertheless, the lifetime values obtained in quaternary mixtures with lower Chol content are longer than in a PSM gel phase and comparable to those obtained in binary POPC/PCer mixtures (Fig. 9B), as well as with those reported for a PSM/PCer-enriched gel phase in ternary POPC/PSM/PCer mixtures

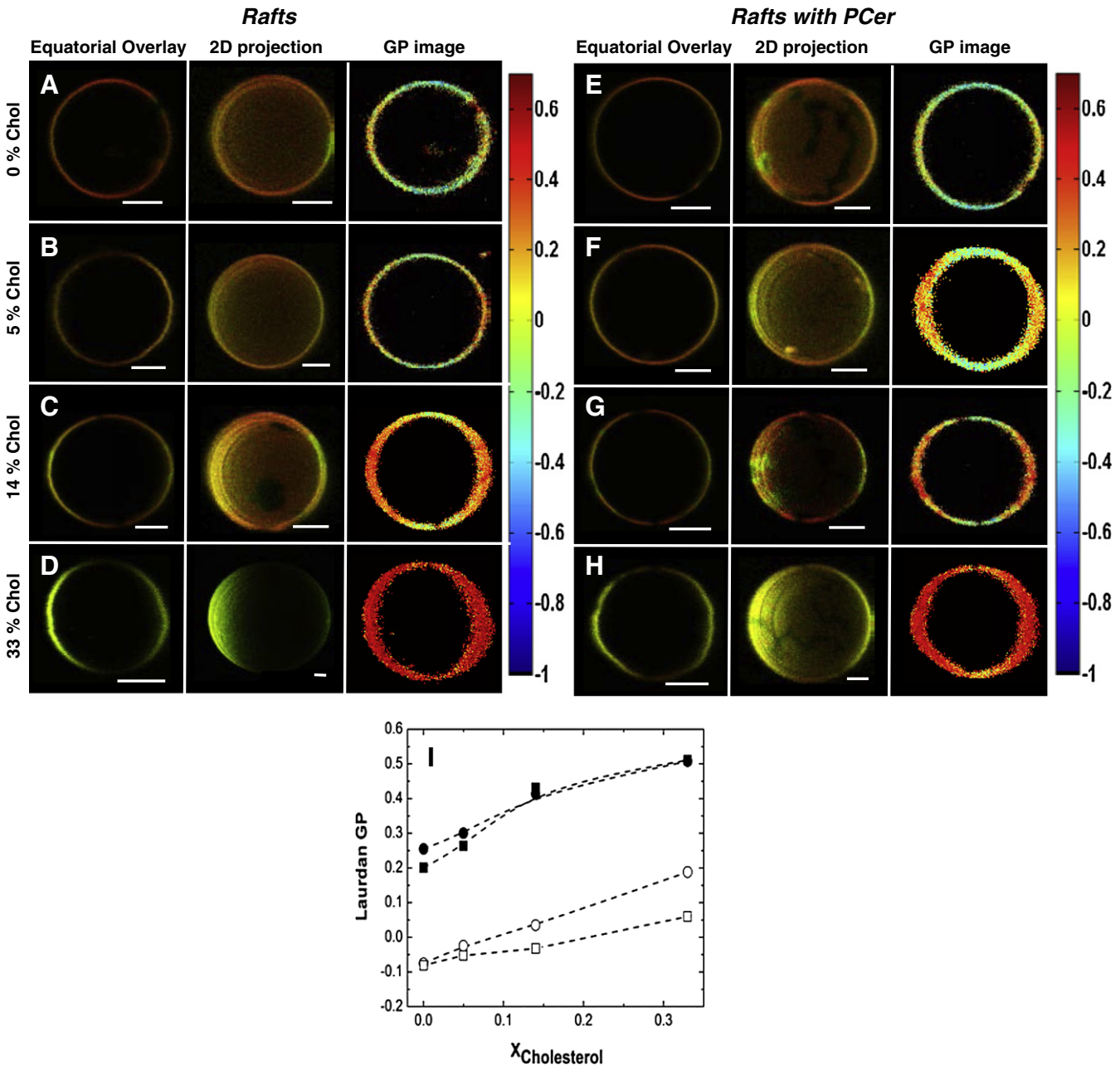

Fig. 8. Two-photon fluorescence microscopy of ternary POPC/PSM/Chol and quaternary POPC/PSM/Chol/PCer mixtures. (A–D) Ternary and (E–H) quaternary mixtures containing (A,E) 0, (B,F) 5, (C,G) 14 and (D,H) 33 mol% of Chol were labeled with Laurdan. Images from the left panel correspond to the overlay of equatorial *z*-section images taken with emission set at 400–460 nm (green channel) and 470–530 nm (red channel). Images from middle panel correspond to the overlay of 2D projection images taken with the same wavelengths described above. The GP images (right panel) were obtained by applying the GP function to the images from green and red channels pixel by pixel. The color scale is from −1 to 0.65. Scale bars correspond to 5 μm. (I) Variation of GP in the ordered phase (closed symbols) and fluid phase (open symbols) in (circles) ternary and (squares) quaternary mixtures, as a function of Chol content. At least 5 different GUVs were evaluated and GP values are the average of all GP images (equatorial *z*-sections) measured for each mixture. SD < 10%.

[25]. The long lifetime component of *t*-PnA fluorescence intensity decay in ternary POPC/Chol/PCer mixtures [33] is similar to the obtained in this study for quaternary mixtures containing a higher Chol fraction, suggesting that the composition and/or properties of the gel phase are comparable in both lipid mixtures. In agreement with our previous studies [33,41], we further highlight the role of the Chol-to-Cer ratio in modulating the biophysical properties of the membranes (Fig. 9C). When the Chol content exceeds that of PCer, a decrease in the long lifetime component of *t*-PnA intensity decay is observed, indicative of a decrease in the packing of the gel phase.

The conclusions aforementioned are further supported by microscopy experiments, where a reduction in the fraction of gel domains is observed as the Chol content of the mixtures is increased. The effect of "generating" Cer in these ternary mixtures is, nevertheless, remarkable and supports a role of membrane structure on Cer-mediated biological processes. Of relevance is the ability of Cer to induce coexistence of 3 phases (l_d, l_o and gel) under physiologically-mimicking conditions, i.e., at intermediate and high Chol fractions. Despite the depletion in PSM, an l_o phase is still present in the mixtures (except for very low Chol content, see Fig. 7), suggesting that formation of Cer in cell membranes may induce a local remodeling of the membrane without a significant effect on other membrane regions.

Our results further show that solely based on the Laurdan GP it is not possible to conclude about the packing properties of the l_o and gel

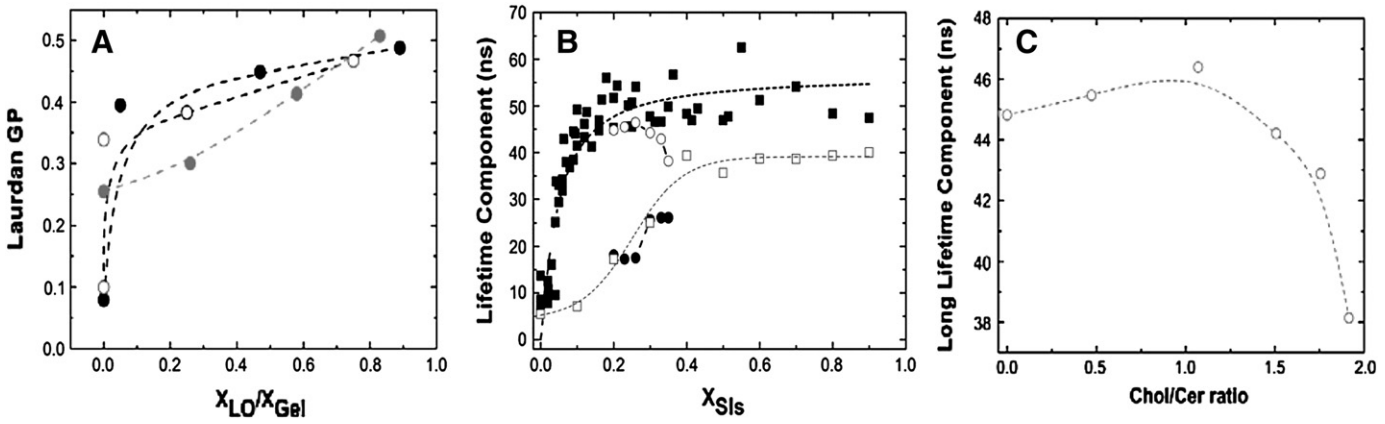

Fig. 9. Properties of the different lipid domains and the interplay between their lipid components. (A) Variation of Laurdan GP values as a function of gel (X_g) and l_o (X_{lo}) phase fraction. The values were taken from (●) POPC/PSM, (○) POPC/DPPC and (●) ternary POPC/PSM/Chol GUVs. At least 5 different GUVs were evaluated and GP values are the average of all GP images (equatorial *z*-sections) measured for each mixture. SD < 10%. (B) Long lifetime component of *t*-PnA intensity decay in (●) ternary and (○) quaternary mixtures as a function of sphingolipid (PSM or PSM + PCer) molar fraction. *t*-PnA long lifetime component is also shown for (■) POPC/PCer and (□) POPC/PSM mixtures. (C) Variation of the long lifetime component of *t*-PnA fluorescence intensity decay as a function of Chol-to-PCer molar ratio in quaternary mixtures. SD < 2%.

phases formed in ternary and quaternary mixtures. This is because the GP values ascribed to the l_o phase containing high Chol are comparable to the values retrieved from PSM- and DPPC-gel phases (Fig. 9A), which might preclude an accurate distinction between these two phases using this probe. Nevertheless, based on the variation of the lifetime and amplitude of the components of *t*-PnA fluorescence intensity decay we suggest that the l_o phase becomes more ordered and the gel phase becomes less packed as the Chol content is increased in quaternary mixtures. Comparing ternary and quaternary mixtures, the fluorescence spectroscopy data would imply that the latter display a less ordered l_o phase. This is a conceivable hypothesis considering that less SM is available to interact with Chol and form an l_o phase and, in addition, it is known that a POPC/Chol-enriched l_o phase is less ordered than a PSM/Chol-enriched l_o phase [18,42].

Comparing data from NBD-DPPE/Rho-DOPE and Laurdan microscopy, we conclude that the later probe is less sensitive to the co-existence of the 3 phases. The main differences reported by Laurdan GP between the ternary and quaternary mixtures reside on the packing properties of the fluid phase, which seems to display a decreased packing in mixtures containing PCer. The reason for this is probably related to the composition of the phases. In the quaternary mixtures, changing the lipid composition not only promotes an alteration in the fraction of the phases but also on their lipid composition. Accordingly, it would not be surprising that in quaternary mixtures containing higher Chol, the fluid phase would be less enriched in Chol since this lipid would be mainly involved in the formation of l_o phase, as demonstrated by the microscopy images obtained with all the probes. In addition, these mixtures are also depleted in PSM which also contributes to a decrease in the order of the fluid disordered phase.

5. Conclusions and biological implications

The present study provides important conclusions concerning i) the distinctive photophysical properties of a set of probes in a variety of lipid mixtures and ii) the characteristics of domains formed by different signaling lipids and their interplay in complex mixtures.

Concerning the first point, we have shown that the partition behavior of the probes and consequently their photophysical properties are dependent on the lipids involved in the formation of the different phases, significantly changing among lipid mixtures even though the same type of phase is formed. The characterization of the photophysical properties of the probes by fluorescence spectroscopy and microscopy in different lipid mixtures, as performed in this study, constitutes an important tool to allow prediction of their phase behavior in more complex lipid mixtures and to select adequate probes to characterize a given mixture or even cell membranes.

Regarding the properties of the phases, this study has shown that sphingolipids are involved in the formation of gel domains that display tighter packing characteristics than phospholipids. Alterations in lipid packing may promote significant changes in cellular processes, for instance, by mediating the partitioning into or exclusion from certain membrane regions [52,53].

We have also reported on the interplay between signaling sphingolipids in more complex lipid mixtures. In particular it was shown that the replacement of PSM by PCer promotes extensive lateral remodeling of the membrane by changing the properties of the phases and by forming PCer-enriched gel domains. In addition, this study provides further insight into the paradigm of Cer–Chol interactions in the membrane. By mimicking the hydrolysis of SM in membranes containing different ratios of SM and Chol, we have shown that the ability of Cer to form tightly-packed gel domains is mediated by Chol and consistent with an increased solubilization of Cer in Chol-enriched l_o phase when Chol levels are high [33,41]. From a biological perspective, these results suggest that Chol/Cer ratio may be a determinant factor in Cer-mediated biological processes. Interestingly, it was reported that cancer cells containing increased levels of Chol were more susceptible to apoptosis upon Chol depletion, suggesting that Cer-mediated apoptosis might be one of the mechanisms activated under low Chol content [54]. Moreover, in some types of tumors the reduction in Cer membrane levels appears to be the mechanism by which tumoral cells can avoid apoptosis [55]. It is therefore plausible to think that the Chol/Cer content is linked to cell survival and could be good targets to promote apoptosis of tumor cells.

Acknowledgements

This work was supported by PTDC/QUI-BIQ/111411/2009 from Fundação para a Ciência e Tecnologia (FCT), Portugal. FCT provided a research grant to S.N. Pinto (SFRH/BD/46296/2008) and F. Fernandes (SFRH/BPD/64320/2009). Alexander Fedorov and L.C. Silva acknowledge funding from Compromisso para a Ciência 2007 and 2008 from FCT. A. H. Futerman is The Joseph Meyerhoff Professor of Biochemistry at the Weizmann Institute of Science.

Appendix A. Supplementary data

Supplementary data to this article can be found online at http://dx.doi.org/10.1016/j.bbamem.2013.05.011.

References

[1] S. Mathias, L.A. Peña, R.N. Kolesnick, Signal transduction of stress via ceramide, Biochem. J. 335 (1998) 465–480.
[2] Y.A. Hannun, L.M. Obeid, Principles of bioactive lipid signalling: lessons from sphingolipids, Nat. Rev. Mol. Cell Biol. 9 (2008) 139–150.
[3] A.G. Lee, Lipid–protein interactions, Biochem. Soc. Trans. 39 (2011) 761–766.
[4] L.A. Bagatolli, Comprehensive Biophysics, Elsevier, 2012.
[5] G. van Meer, D.R. Voelker, G.W. Feigenson, Membrane lipids: where they are and how they behave, Nat. Rev. Mol. Cell Biol. 9 (2008) 112–124.
[6] L.J. Pike, Lipid rafts: heterogeneity on the high seas, Biochem. J. 378 (2004) 281–292.
[7] H. Grassmé, V. Jendrossek, J. Bock, A. Riehle, E. Gulbins, Ceramide-rich membrane rafts mediate CD40 clustering, J. Immunol. 168 (2002) 298–307.
[8] R.F.M. de Almeida, L.M.S. Loura, M. Prieto, Membrane lipid domains and rafts: current applications of fluorescence lifetime spectroscopy and imaging, Chem. Phys. Lipids 157 (2009) 61–77.
[9] J.M. Holopainen, H.L. Brockman, R.E. Brown, P.K. Kinnunen, Interfacial interactions of ceramide with dimyristoylphosphatidylcholine: impact of the N-acyl chain, Biophys. J. 80 (2001) 765–775.
[10] P.K.J. Kinnunen, J.M. Holopainen, Sphingomyelinase activity of LDL: a link between atherosclerosis, ceramide, and apoptosis? Trends Cardiovasc. Med. 12 (2002) 37–42.
[11] L. Silva, R.F.M. de Almeida, A. Fedorov, A.P.a Matos, M. Prieto, Ceramide-platform formation and -induced biophysical changes in a fluid phospholipid membrane, Mol. Membr. Biol. 23 (2006) 137–148.
[12] J.V. Busto, M.L. Fanani, L. De Tullio, J. Sot, B. Maggio, F.M. Goñi, A. Alonso, Coexistence of immiscible mixtures of palmitoylsphingomyelin and palmitoylceramide in monolayers and bilayers, Biophys. J. 97 (2009) 2717–2726.
[13] S. Munro, Lipid rafts: elusive or illusive? Cell 115 (2003) 377–388.
[14] B. Nichols, Cell biology: without a raft, Nature 436 (2005) 638–639.
[15] A.S. Shaw, Lipid rafts: now you see them, now you don't, Nat. Immunol. 7 (2006) 1139–1142.
[16] S.A. Sanchez, M.A. Tricerri, E. Gratton, Laurdan generalized polarization fluctuations measures membrane packing micro-heterogeneity in vivo, Proc. Natl. Acad. Sci. U. S. A. 109 (2012) 7314–7319.
[17] F. Gallyas, O. Farkas, M. Mázló, Gel-to-gel phase transition may occur in mammalian cells: mechanism of formation of "dark" (compacted) neurons, Biol. Cell 96 (2004) 313–324.
[18] F. Aresta-Branco, A.M. Cordeiro, H.S. Marinho, L. Cyrne, F. Antunes, R.F.M. de Almeida, Gel domains in the plasma membrane of *Saccharomyces cerevisiae*: highly ordered, ergosterol-free, and sphingolipid-enriched lipid rafts, J. Biol. Chem. 286 (2011) 5043–5054.
[19] S.N. Pinto, L.C. Silva, A.H. Futerman, M. Prieto, Effect of ceramide structure on membrane biophysical properties: the role of acyl chain length and unsaturation, Biochim. Biophys. Acta 1808 (2011) 2753–2760.
[20] S.N. Pinto, L.C. Silva, R.F.M. De Almeida, M. Prieto, R.F.M. de Almeida, Membrane domain formation, interdigitation, and morphological alterations induced by the very long chain asymmetric C24:1 ceramide, Biophys. J. 95 (2008) 2867–2879.
[21] T. Parasassi, G. De Stasio, G. Ravagnan, R.M. Rusch, E. Gratton, Quantitation of lipid phases in phospholipid vesicles by the generalized polarization of Laurdan fluorescence, Biophys. J. 60 (1991) 179–189.
[22] F.M. Harris, K.B. Best, J.D. Bell, Use of Laurdan fluorescence intensity and polarization to distinguish between changes in membrane fluidity and phospholipid order, Biochim. Biophys. Acta 1565 (2002) 123–128.
[23] T. Parasassi, E.K. Krasnowska, L.A. Bagatolli, E. Gratton, Laurdan and prodan as polarity-sensitive fluorescent membrane probes, J. Fluoresc. 8 (1998) 365–373.
[24] B.M. Stott, M.P. Vu, C.O. McLemore, M.S. Lund, E. Gibbons, T.J. Brueseke, H.A. Wilson-Ashworth, J.D. Bell, Use of fluorescence to determine the effects of cholesterol on lipid behavior in sphingomyelin liposomes and erythrocyte membranes, J. Lipid Res. 49 (2008) 1202–1215.
[25] B.M. Castro, R.F.M. de Almeida, L.C. Silva, A. Fedorov, M. Prieto, Formation of ceramide/sphingomyelin gel domains in the presence of an unsaturated phospholipid: a quantitative multiprobe approach, Biophys. J. 93 (2007) 1639–1650.
[26] D.M. Owen, C. Rentero, A. Magenau, A. Abu-Siniyeh, K. Gaus, Quantitative imaging of membrane lipid order in cells and organisms, Nat. Protoc. 7 (2011) 24–35.
[27] T.F. Martin, Phosphoinositide lipids as signaling molecules: common themes for signal transduction, cytoskeletal regulation, and membrane trafficking, Annu. Rev. Cell Dev. Biol. 14 (1998) 231–264.
[28] H. Grassmé, J. Riethmüller, E. Gulbins, Biological aspects of ceramide-enriched membrane domains, Prog. Lipid Res. 46 (2007) 161–170.
[29] L.C. Silva, R.F.M. de Almeida, B.M. Castro, A. Fedorov, M. Prieto, Ceramide-domain formation and collapse in lipid rafts: membrane reorganization by an apoptotic lipid, Biophys. J. 92 (2007) 502–516.
[30] B.R. Lentz, Y. Barenholz, T.E. Thompson, Fluorescence depolarization studies of phase transitions and fluidity in phospholipid bilayers 1 single component phosphatidylcholine liposomes, Biochemistry 15 (1976) 4529–4537.
[31] L.A. Sklar, G.P. Miljanich, E.A. Dratz, Phospholipid lateral phase separation and the partition of cis-parinaric acid and trans-parinaric acid among aqueous, solid lipid, and fluid lipid phases, Biochemistry 18 (1979) 1707–1716.
[32] R.F.M. de Almeida, L.M.S. Loura, A. Fedorov, M. Prieto, Lipid rafts have different sizes depending on membrane composition: a time-resolved fluorescence resonance energy transfer study, J. Mol. Biol. 346 (2005) 1109–1120.
[33] B.M. Castro, L.C. Silva, A. Fedorov, R.F.M. de Almeida, M. Prieto, Cholesterol-rich fluid membranes solubilize ceramide domains: implications for the structure and dynamics of mammalian intracellular and plasma membranes, J. Biol. Chem. 284 (2009) 22978–22987.
[34] T. Parasassi, E. Gratton, W.M. Yu, P. Wilson, M. Levi, Two-photon fluorescence microscopy of Laurdan generalized polarization domains in model and natural membranes, Biophys. J. 72 (1997) 2413–2429.
[35] L.A. Bagatolli, T. Parasassi, G.D. Fidelio, E. Gratton, A model for the interaction of 6-lauroyl-2-(N, N-dimethylamino)naphthalene with lipid environments: implications for spectral properties, Photochem. Photobiol. 70 (1999) 557–564.
[36] T. Parasassi, G. Ravagnan, R.M. Rusch, E. Gratton, Modulation and dynamics of phase properties in phospholipid mixtures detected by Laurdan fluorescence, Photochem. Photobiol. 57 (1993) 403–410.
[37] M.L. Schmidt, L. Ziani, M. Boudreau, J.H. Davis, Phase equilibria in DOPC/DPPC: conversion from gel to subgel in two component mixtures, Methods (2009) 1–11.
[38] L. Li, J.-X. Cheng, Coexisting stripe- and patch-shaped domains in giant unilamellar vesicles, Biochemistry 45 (2006) 11819–11826.
[39] R. Koynova, M. Caffrey, Phases and phase transitions of the sphingolipids, Biochim. Biophys. Acta 1255 (1995) 213–236.
[40] M. Fidorra, T. Heimburg, L.A. Bagatolli, Direct visualization of the lateral structure of porcine brain cerebrosides/POPC mixtures in presence and absence of cholesterol, Biophys. J. 97 (2009) 142–154.
[41] L.C. Silva, A.H. Futerman, M. Prieto, Lipid raft composition modulates sphingomyelinase activity and ceramide-induced membrane physical alterations, Biophys. J. 96 (2009) 3210–3222.
[42] H. Kaiser, D. Lingwood, I. Levental, J.L. Sampaio, L. Kalvodova, L. Rajendran, K. Simons, Order of lipid phases in model and plasma membranes, PNAS 106 (2009) 16645–16650.
[43] G. Staneva, A. Momchilova, C. Wolf, P.J. Quinn, K. Koumanov, Membrane microdomains: role of ceramides in the maintenance of their structure and functions, Biochim. Biophys. Acta 1788 (2009) 666–675.
[44] L.A. Bagatolli, E. Gratton, Two photon fluorescence microscopy of coexisting lipid domains in giant unilamellar vesicles of binary phospholipid mixtures, Biophys. J. 78 (2000) 290–305.
[45] L.A. Bagatolli, E. Gratton, G.D. Fidelio, Water dynamics in glycosphingolipid aggregates studied by Laurdan fluorescence, Biophys. J. 75 (1998) 331–341.
[46] A.E.P. Bastos, H.S. Marinho, A.M. Cordeiro, A.M. de Soure, R.F.M. de Almeida, Biophysical properties of ergosterol-enriched lipid rafts in yeast and tools for their study: characterization of ergosterol/phosphatidylcholine membranes with three fluorescent membrane probes, Chem. Phys. Lipids 165 (2012) 577–588.
[47] P.R. Maulik, G.G. Shipley, Interactions of N-stearoyl sphingomyelin with cholesterol and dipalmitoylphosphatidylcholine in bilayer membranes, Biophys. J. 70 (1996) 2256–2265.
[48] R.F.M. de Almeida, A. Fedorov, M. Prieto, Sphingomyelin/phosphatidylcholine/cholesterol phase diagram: boundaries and composition of lipid rafts, Biophys. J. 85 (2003) 2406–2416.
[49] E.R. Catapano, L.R. Arriaga, G. Espinosa, F. Monroy, D. Langevin, I. López-Montero, Solid character of membrane ceramides: a surface rheology study of their mixtures with sphingomyelin, Biophys. J. 101 (2011) 2721–2730.
[50] G. Espinosa, I. López-Montero, F. Monroy, D. Langevin, Shear rheology of lipid monolayers and insights on membrane fluidity, Proc. Natl. Acad. Sci. U. S. A. 108 (2011) 6008–6013.
[51] E. Gulbins, S. Dreschers, B. Wilker, H. Grassmé, Ceramide, membrane rafts and infections, J. Mol. Med. 82 (2004) 357–363.
[52] Y. Pewzner-Jung, H. Park, E.L. Laviad, L.C. Silva, S. Lahiri, J. Stiban, R. Erez-Roman, B. Brügger, T. Sachsenheimer, F. Wieland, M. Prieto, A.H. Merrill, A.H. Futerman, A critical role for ceramide synthase 2 in liver homeostasis: I alterations in lipid metabolic pathways, J. Biol. Chem. 285 (2010) 10902–10910.
[53] L.C. Silva, O. Ben David, Y. Pewzner-Jung, E.L. Laviad, J. Stiban, S. Bandyopadhyay, A.H. Merrill, M. Prieto, A.H. Futerman, Ablation of ceramide synthase 2 strongly affects biophysical properties of membranes, J. Lipid Res. 53 (2012) 430–436.
[54] Y.C. Li, M.J. Park, S.-K. Ye, C.-W. Kim, Y.-N. Kim, Elevated levels of cholesterol-rich lipid rafts in cancer cells are correlated with apoptosis sensitivity induced by cholesterol-depleting agents, Am. J. Pathol. 168 (2006) 1107–1118.
[55] W.-C. Huang, C.-L. Chen, Y.-S. Lin, C.-F. Lin, Apoptotic sphingolipid ceramide in cancer therapy, J. Lipids 2011 (2011) 1–15.